Biophysical Journal Volume 74 January 1998 319–327

Permeation of Halide Anions through Phospholipid Bilayers Occurs by the Solubility-Diffusion Mechanism

S. Paula, A. G. Volkov, and D. W. Deamer

Department of Chemistry and Biochemistry, University of California, Santa Cruz, California 95064 USA

ABSTRACT Two alternative mechanisms are frequently used to describe ionic permeation of lipid bilayers. In the first, ions partition into the hydrophobic phase and then diffuse across (the solubility-diffusion mechanism). The second mechanism assumes that ions traverse the bilayer through transient hydrophilic defects caused by thermal fluctuations (the pore mechanism). The theoretical predictions made by both models were tested for halide anions by measuring the permeability coefficients for chloride, bromide, and iodide as a function of bilayer thickness, ionic radius, and sign of charge. To vary the bilayer thickness systematically, liposomes were prepared from monounsaturated phosphatidylcholines (PC) with chain lengths between 16 and 24 carbon atoms. The fluorescent dye MQAE (*N*-(ethoxycarbonylmethyl)-6-methoxyquinolinium bromide) served as an indicator for halide concentration inside the liposomes and was used to follow the kinetics of halide flux across the bilayer membranes. The observed permeability coefficients ranged from 10^{-9} to 10^{-7} cm/s and increased as the bilayer thickness was reduced. Bromide was found to permeate approximately six times faster than chloride through bilayers of identical thickness, and iodide permeated three to four times faster than bromide. The dependence of the halide permeability coefficients on bilayer thickness and on ionic size were consistent with permeation of hydrated ions by a solubility-diffusion mechanism rather than through transient pores. Halide permeation therefore differs from that of a monovalent cation such as potassium, which has been accounted for by a combination of the two mechanisms depending on bilayer thickness.

INTRODUCTION

The permeation process by which ions and small polar molecules cross phospholipid bilayers is commonly interpreted in terms of two alternative theories: the solubility-diffusion mechanism and the pore mechanism. Solubility-diffusion satisfactorily describes the permeation of many solutes, including water itself (Finkelstein, 1987) while permeation through transient pores in the bilayer is the dominant pathway for cations under certain circumstances (Deamer and Volkov, 1995). For other species, such as the anions thiocyanate and perchlorate, there is evidence which strongly supports the solubility-diffusion mechanism (Dilger et al., 1979). An effective strategy to test a given permeation mechanism is to measure the permeability coefficient as a function of a parameter that can be varied experimentally. One such parameter is the bilayer thickness, in that the solubility-diffusion mechanism and the pore mechanism have a markedly different dependence on bilayer thickness and therefore can be distinguished (Paula et al., 1996). Other useful parameters that discriminate between the two mechanisms for both cations and anions are the radius of the permeating ion and the sign of charge. In either case, the theoretical predictions are sufficiently different from each other so that a decision in favor of one mechanism or the other becomes possible by comparing the mechanism-specific expectations to the experimental findings.

We therefore measured the permeability coefficients of chloride, bromide, and iodide as a function of bilayer thickness. The experimental results were compared with theoretical expectations from the solubility-diffusion mechanism and the pore mechanism, and with earlier results for cations (Paula et al., 1996). This approach allowed us to address the following questions:

1. What is the effect of bilayer thickness and ionic size on the relative permeability of halide anions? According to the pore model, the dependence of the permeability coefficient on bilayer thickness should be pronounced, and the coefficient is expected to decrease with increasing bare ionic radius. In contrast, the solubility-diffusion mechanism predicts only a modest dependence of permeability on bilayer thickness, and the permeability coefficient is expected to increase in the order $P_{Cl} < P_{Br} < P_I$.
2. Do anions permeate as bare ions or as hydrated species? Both the solubility-diffusion and pore mechanism make testable predictions that help answer this question. For instance, if anions permeate as bare ions, the permeability coefficients of chloride, bromide, and iodide should differ by several orders of magnitude if the solubility-diffusion mechanism is correct.
3. How does halide anion permeation compare to that of monovalent cations such as potassium and protons? The solubility-diffusion mechanism allows anions to permeate faster than cations of the same size. The pore mechanism, on the other hand, predicts that cations should permeate faster than anions.

Received for publication 19 May 1997 and in final form 2 October 1997.

Address reprint requests to Dr. Stefan Paula, Dept. of Chemistry and Biochemistry, University of California at Santa Cruz, Santa Cruz, CA 95064. Tel.: 408-459-3061; Fax: 408-459-5158; E-mail: stefan@chemistry.ucsc.edu.

0006-3495/98/01/319/09 $2.00

MATERIALS AND METHODS

Chemicals

All phospholipids were obtained from Avanti polar lipids (Alabaster, AL). The lipids were monounsaturated phosphatidylcholines (PC) with a *cis* double bond located at the center of each hydrocarbon chain which permitted measurements in the liquid-crystalline phase at 30°C. The length of the hydrocarbon chains ranged from 16 to 24 carbon atoms (palmitoleoyl-PC, oleoyl-PC, eicosenoyl-PC, erucoyl-PC, and nervonoyl-PC). The fluorescent dye MQAE (*N*-(ethoxycarbonylmethyl)-6-methoxyquinolinium bromide) was purchased from Molecular Probes (Eugene, OR). All other chemicals were obtained from Sigma (St. Louis, MO) and used without further purification.

Liposome preparation

Liposomes were prepared by the extrusion method (Hope et al., 1985) using polycarbonate filters with a pore diameter of 200 nm (Nucleopore, Pleasanton, CA). The buffer in which the liposomes were prepared was a mixture of 20 mM HEPES (*N*-2-hydroxyethlypiperazine-*N*′-ethanesulfonic acid), 200 mM potassium gluconate, and 10 mM MQAE, pH 7.4. External dye was removed by passing the liposomes over a size exclusion column (G-25) that had been equilibrated with isoosmotic, dye-free buffer (20 mM HEPES, 210 mM potassium gluconate). The liposome mean diameter was measured by quasi-elastic light scattering with a BI-90 analyzer (Brookhaven Instruments Corp., Holtsville, NY).

Anion flux measurements

Anion fluxes across lipid bilayers were measured by fluorescence spectroscopy according to a procedure that was developed by Verkman et al. for the study of chloride permeation in liposomes and cells (Verkman et al., 1989a; Verkman, 1990). This method utilizes the fluorescence signal of the dye MQAE, which is quenched by chloride via a collisional quenching mechanism. Since MQAE is also sensitive to bromide and iodide, the technique could be utilized to observe the permeation process of these two ions in an analogous way.

After the dye was encapsulated inside the liposomes as described above, halide flux across the bilayer was initiated by diluting 50 μl of the liposome stock solution (10 mg/ml) into 3 ml of isoosmotic buffer solution in which 50 mM potassium gluconate had been replaced by 50 mM chloride, bromide, or iodide. All measurements were performed in a stirred cuvette with temperature kept at 30°C. Before starting the experiments, 3.5 μM valinomycin was added to prevent the development of an electrostatic transmembrane potential that would have restricted the unhindered movement of the anions across the bilayer.

The time course of the dye fluorescence in response to the dissipation of the halide gradient was monitored by an Aminco SLM 8000 fluorimeter (SLM Instruments, IL). The dye was excited at a wavelength of 354 nm and its emission was detected at 450 nm. At the end of each measurement, 5 μM ionophore tributyltin chloride (TBT) was added to the sample. TBT immediately collapsed any remaining halide gradient, thereby providing a calibration of fluorescence intensity at a halide concentration of 50 mM.

The fluorescence versus time curves were converted into concentration versus time profiles using the following equations:

$$c(t) = \frac{FU_0 - FU_\infty}{K_Q(FU(t) - FU_\infty)} - \frac{1}{K_Q} \quad (1)$$

$$FU_\infty = \frac{FU_{50}(1 + 0.050\,K_Q) - FU_0}{0.050\,K_Q} \quad (2)$$

Here, FU_0 and FU_{50} were the fluorescence intensities measured at 0 mM and 50 mM quencher concentration, respectively. FU_0 equaled the fluorescence intensity immediately after the injection of the liposomes and FU_{50} was the intensity after the addition of TBT. FU_∞ was the calculated static background fluorescence intensity that was not susceptible to quenching and originated from processes such as light scattering by the liposomes or electronic noise of the photomultiplier. K_Q was the Stern-Volmer quenching constant which serves as a measure of the sensitivity of a fluorescent dye to a specific quencher (Lakowicz, 1983). It was determined in separate experiments as described below. $FU(t)$ was the experimentally observed fluorescence signal measured at time t, and $c(t)$ was the corresponding halide concentration inside the liposomes at that time.

The concentration curves obtained from Eqs. 1 and 2 were fitted to a single-exponential rise. The first derivative of the fit at time 0 gave the permeability coefficient P according to the following relation:

$$P = \left(\frac{dc}{dt}\right)_{t=0} \frac{r}{3\Delta c_{t=0}} \quad (3)$$

where r was the mean hydrodynamic radius of the liposomes as determined from quasi-elastic light scattering and Δc was the initial concentration gradient of 50 mM for all experiments.

Determination of the quenching constants

For quantitative evaluation of the fluorescence data, the Stern-Volmer quenching constants K_Q had to be determined for each halide. This was done in a separate set of fluorimetric titration experiments in which 0.1 mM MQAE was titrated with small aliquots of concentrated halide solution (1 M of the respective potassium salt) and the resulting changes in fluorescence intensity were recorded. The titrations were performed in the same buffer solution that was used to make the liposomes. After correction for dilution, the quenching constants were obtained from a linear fit of the fluorescence intensity data to the well-known Stern-Volmer equation:

$$FU(0)/FU([Q]) = 1 + K_Q[Q] \quad (4)$$

where $[Q]$ was the halide concentration in the sample and $FU(0)$ and $FU([Q])$ were the observed fluorescence intensities of the dye in the absence and the presence of quencher molecules, respectively.

RESULTS

Stern-Volmer plots for MQAE

Stern-Volmer plots for the fluorimetric titration of MQAE are shown in Fig. 1. The solid lines were obtained from linear regression analysis and gave the following quenching constants: K_Q (Cl) = 45.7 M^{-1}, K_Q (Br) = 67.8 M^{-1}, K_Q (I) = 111.8 M^{-1}. The values for the Stern-Volmer constants reported here are smaller than previously published by Verkman (45.7 M^{-1} versus 200 M^{-1} for chloride, 67.8 M^{-1} versus 293 M^{-1} for bromide, and 111.8 M^{-1} versus 456 M^{-1} for iodide, Verkman et al., 1989a). This apparent discrepancy results from differences in the buffer composition in which the measurements were performed (5 mM phosphate versus 20 mM HEPES/200 mM potassium gluconate). Because the actual values for quenching constants are sensitive to the local environment of the fluorescent probe, such as the ionic strength, differences in the results for the quenching constants are expected. That is, the collision rate of the negatively charged quencher ions with the positively charged dye will decrease if the ionic strength of solution is raised, and the quenching constants will be lower. This conclusion was confirmed by control experiments in which the HEPES/gluconate buffer system was

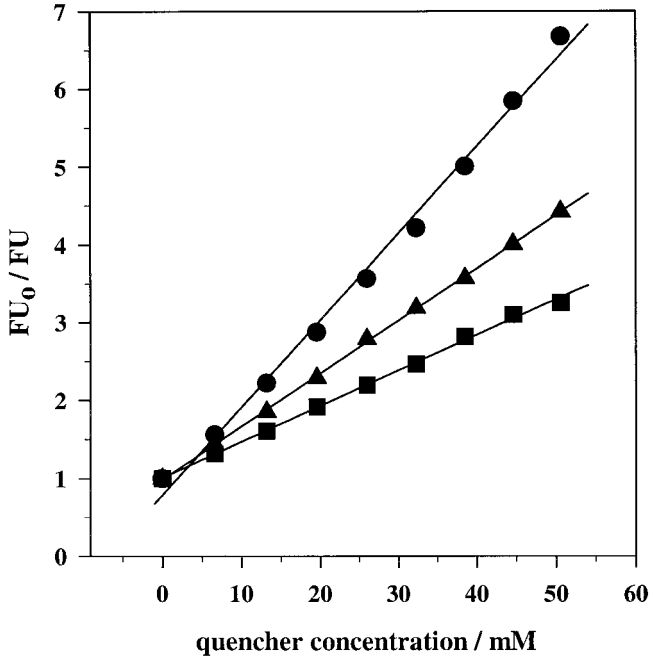

FIGURE 1 Stern-Volmer plots for the fluorimetric titrations of MQAE (λ_{ex} = 354 nm, λ_{em} = 450 nm) with 1 M KCl (■), KBr (▲), and KI (●). Titrations were carried out in 200 mM potassium gluconate/20 mM HEPES (pH 7.4). Solid lines were obtained from linear regression and gave the following quenching constants: K_Q (Cl) = 45.7 M^{-1}, K_Q (Br) = 67.8 M^{-1}, and K_Q (I) = 111.8 M^{-1}.

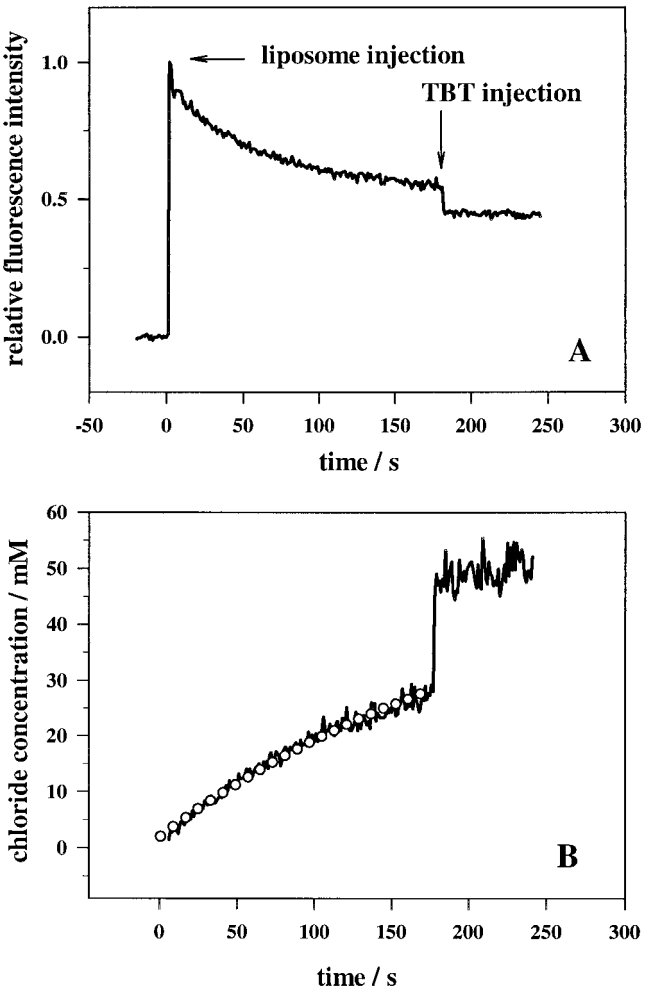

FIGURE 2 Time course of a typical chloride permeation experiment. Liposomes (10 mg/ml) composed of dioleoyl-PC were prepared in 210 mM potassium gluconate and 20 mM HEPES (pH 7.4). The internal MQAE concentration was 10 mM. At the time indicated, a 5 μl aliquot of liposome stock solution was diluted into 3 ml buffer containing 50 mM potassium chloride, 160 mM potassium gluconate, 20 mM HEPES (pH 7.4), and 3.5 μM valinomycin. The ionophore TBT (5 μM) was added at the end of the experiment to calibrate the signal. (*A*) Original fluorescence trace. (*B*) Time dependence of internal chloride concentration as obtained from the fluorescence curve. The symbols (○) represent a single exponential fit to the data.

replaced by the phosphate buffer used by Verkman et al. Under these conditions, the quenching constants matched perfectly.

Chloride permeation measurements

The time course of a typical chloride permeation experiment is shown in Fig. 2. At zero time, liposomes were diluted into buffer containing 50 mM potassium chloride (Fig. 2 *A*). Over a period of 150 s, the MQAE fluorescence was quenched as chloride diffused into the liposome interior. The chloride ionophore TBT was added at the end of the experiment to calibrate the signal by allowing chloride to equilibrate freely across the bilayer. Fig. 2 *B* shows the time dependence of the internal chloride concentration calculated from the fluorescence standard curve for chloride given in Fig. 1. The symbols represent a single exponential fit to the data.

Comparison of chloride, bromide, and iodide permeation

Similar experiments were performed for bromide and iodide, and the anion permeability coefficients observed for the various lipids are summarized in Table 1 and Fig. 3. Each value represents the average of five measurements. In the case of iodide, which permeates rapidly, the permeability coefficients could only be measured reliably for the two longest lipids within the limits of the time resolution of the experimental setup. The results of the measurements covered the range between 10^{-9} and 10^{-7} cm/s.

The permeability coefficient for chloride is always lower than the corresponding coefficient for bromide. On average, the difference amounts to a factor of six, depending slightly on the actual chain length. Iodide always permeates faster than the other two halides. The difference between bromide and iodide is roughly three- to fourfold.

Effect of bilayer thickness on permeation rates

Fig. 3 also shows that the measured permeability coefficient for any of the halides is clearly a function of bilayer thick-

TABLE 1 Permeability coefficients for chloride, bromide, and iodide as measured for five different lipid chain lengths

d [Å]	$P_{Chloride} \cdot 10^9$ [cm/s]	$P_{Bromide} \cdot 10^8$ [cm/s]	$P_{Iodide} \cdot 10^8$ [cm/s]
23.5	28.2 ± 14.5	9.76 ± 3.77	—
27.0	12.1 ± 1.40	7.44 ± 2.00	—
30.5	6.04 ± 2.24	2.40 ± 0.16	—
34.0	4.17 ± 0.87	3.04 ± 0.68	12.4 ± 2.80
37.5	1.87 ± 0.54	1.54 ± 0.65	3.90 ± 0.76

Each entry represents the average of five repeats and the standard deviation. d is the thickness of the hydrophobic region of the bilayer (Lewis and Engelman, 1983).

ness. P decreases as the chain length of the lipids is increased. The difference in permeability coefficients between longest and shortest lipid is ~15-fold in the case of chloride and ~6-fold in the case of bromide. Within experimental error, the increments by which the logarithm of P decreases from one lipid to the next seem to remain constant within a series.

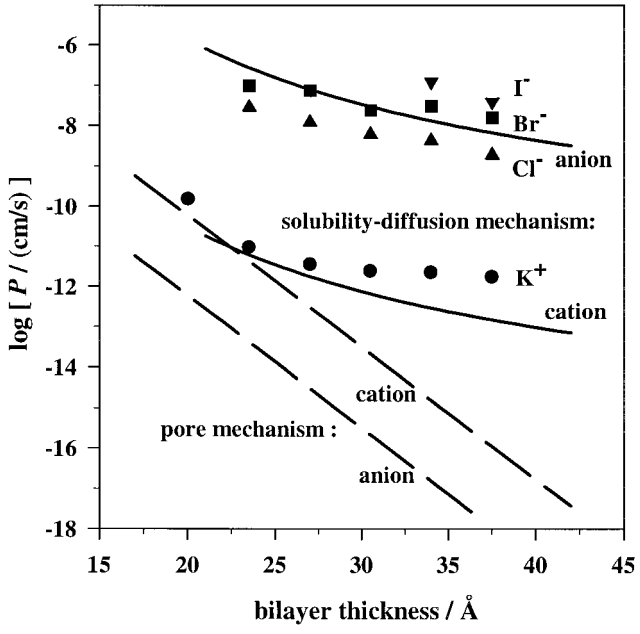

FIGURE 3 Dependence of P on bilayer thickness. Experimentally obtained permeability coefficients of chloride (▲), bromide (■), and iodide (▼) as a function of thickness of the hydrophobic region of the bilayer on a semilogarithmic scale. Reference data for potassium (●) were included for comparison (Paula et al., 1996). The upper solid line was calculated for an anion permeating by the solubility-diffusion mechanism; the lower solid line is the corresponding curve for a cation of the same size. The dashed line was computed according to the pore mechanism for an anion and a cation of unhydrated radius 1.6 Å, respectively. Parameters: $r(K^+) = 1.49$ Å, $r(Cl^-) = 1.64$ Å, $r(Br^-) = 1.80$ Å, $r(I^-) = 2.05$ Å, $r(K^+$, hydrated) = $r(Cl^-$, hydrated) = $r(I^-$, hydrated) = 3.31 Å, $\epsilon_w = 78$, $\epsilon_{hc} = 2$, $\gamma_{w/hc} = 35$ mN m^{-1}, $\Delta\phi = -150$ mV, $D = 2 \cdot 10^{-5}$ cm^2 s^{-1}, σ (cation) = 10, σ (anion) = 0.1, $R_v = 1.05 \cdot 10^{-6}$ cm, $A = 26{,}000$ cm^{-1}, $n_o = 1.04 \cdot 10^{29}$ cm^5, $T = 303.15$ K, $k_1 = 2.2 \cdot 10^{15}$ kJ mol^{-1} cm^{-2}, $k_2 = 1.9 \cdot 10^8$ kJ mol^{-1} cm^{-1}.

DISCUSSION

Due to the biological importance of chloride transport across membranes, literature data for chloride permeability coefficients are plentiful. The earliest studies in liposomes were carried out by radioactive labeling techniques in small unilamellar liposomes prepared by sonication (Hauser et al., 1973; Nicholls and Miller, 1974; Toyoshima and Thompson, 1975). These data were later complemented by conductivity measurements in planar bilayer membranes (Gutknecht et al., 1978). A few years ago, chloride-sensitive fluorescent dyes were introduced that permitted measurements with significantly improved time resolution and small amounts of sample material (Verkman et al., 1989a, b; Verkman, 1990). The overall results of these studies vary considerably and seem to depend strongly on the technique employed, the lipid composition of the bilayers, the preparation method of the bilayer, and experimental conditions such as temperature, ionic strength, pH, etc. Reported values for the permeability coefficient of chloride in liposomes are as high as 10^{-8} cm/s and as low as 10^{-11} cm/s. Results from studies in planar bilayers are generally somewhat higher than those in liposomes, which is often ascribed to the differences between these two experimental approaches (curvature of the bilayer, traces of organic solvents present in planar bilayers, etc.). The results of our study ($3 \cdot 10^{-8}$-$2 \cdot 10^{-9}$ cm/s) are well within the upper half of the range of the reported values.

In contrast to chloride, reference data for bromide and iodide are very limited. Gutknecht et al. (1978) studied bromide permeation in planar bilayer systems composed of egg lecithin and a long-chain secondary amine, and reported a permeability coefficient of $5.5 \cdot 10^{-6}$ cm/s at pH 7.4. This value is one to two orders of magnitude higher than the data of our study. Given the differences in lipid composition (egg lecithin and a secondary amine versus pure PC) and lipid systems (planar bilayers versus liposomes), the deviation seems to be within a reasonable limit.

We will now examine the experimental evidence to determine the most plausible permeation mechanism. The two alternatives that will be considered are the solubility-diffusion mechanism and the pore mechanism. A reasonable mechanism must reflect the two major experimental characteristics correctly by accounting for the dependence of P on bilayer thickness and by explaining how an increase in the unhydrated ionic radius effects P.

In addition to the experimental data described in this study, we will also consider earlier results obtained for potassium permeation in identical bilayer systems (Paula et al., 1996). As shown in Fig. 3, potassium ions permeate slower than halides by two to three orders of magnitude, despite a comparable hydrated ionic radius (3.31 Å) and a bare radius (1.49 Å) which is ~10% lower than that of chloride (1.64 Å) and ~30% lower than that of iodide (2.05 Å) (Conway, 1981). The favored permeation mechanism must also account for the difference between cation and anion permeability coefficients.

The solubility-diffusion mechanism

The solubility-diffusion mechanism has been used extensively to describe water permeation through lipid bilayers (Finkelstein, 1987; Marrink and Berendsen, 1994), but can be applied to the permeation of many other species as well. According to this mechanism, the lipid bilayer is pictured as a thin slab of a hydrophobic medium that separates two aqueous phases and acts as a diffusion barrier. In order to get from one aqueous phase into the other, the permeant must dissolve into the hydrophobic phase, diffuse across it, and dissolve into the second aqueous phase.

In the following paragraphs we will show what predictions this mechanism makes regarding the dependence of P on ionic radius, bilayer thickness, and sign of charge of the permeating ion. Applying Fick's first law of diffusion, one can derive the following expression for the permeability coefficient P (Hauser et al., 1973; Finkelstein, 1987; Gennis, 1989):

$$P = \frac{KD}{d}. \tag{5}$$

Here, D is the diffusion coefficient of the permeating particle in the hydrophobic phase which is commonly approximated by its diffusion coefficient in water. The thickness of the hydrophobic region of the bilayer is represented by d and can be obtained from x-ray diffraction studies (Lewis and Engelman, 1983). K stands for the partition coefficient of the ion between water and the hydrophobic interior of the bilayer. K can be calculated from the change in Gibbs free energy, ΔG, that is associated with the transfer of the ion from water into the hydrocarbon phase (Markin and Volkov, 1989; Israelachvili, 1992). If only interactions between the ion and solvent molecules are included in ΔG, the reference state of ΔG is the state of infinite dilution and the calculated partition coefficient will therefore be in mole fraction units (Gurney, 1953; Tanford, 1980). Since K must be expressed in molarities to be compatible with Eq. 5, it must be converted into molarities using the molar volumes of water ($\bar{V}_w$) and the hydrophobic solvent ($\bar{V}_{hc}$). It should be noted that this conversion is equivalent to using one-molar solutions as reference states and adding to the obtained configurational Gibbs free energy, ΔG_{config}, the contribution arising from the change in the entropy of mixing, ΔS_{mix}, that occurs if the ions are transferred between two systems that contain a different number of solvent molecules. For sufficiently diluted solutions, K can be obtained from the following equation:

$$K = \frac{\bar{V}_w}{\bar{V}_{hc}} \exp\left[\frac{-\Delta G}{RT}\right] = \exp\left[\frac{-\Delta G_{config} + T\Delta S_{mix}}{RT}\right]. \tag{6}$$

Knowing both the thickness of the hydrophobic region, d, and the area occupied by a lipid molecule (70 Å^2; Small, 1967), $\bar{V}_{hc}$ can be estimated.

The total Gibbs free energy of transfer for an ion can be written as the sum of several energy terms that include electrostatic, hydrophobic, and specific contributions (Ketterer et al., 1971; Flewelling and Hubbell, 1986b).

$$\Delta G = \Delta G_B + \Delta G_I + \Delta G_D + \Delta G_H + \Delta G_{SP} \tag{7}$$

The first term, ΔG_B, is the classical Born energy, which accounts for the electrostatic energy required to remove an ion of radius r and charge q from the aqueous phase (dielectric constant = ϵ_w) and place it in a hydrophobic solvent whose dielectric constant ϵ_{hc} resembles that of the bilayer interior (Born, 1920). According to this model, the solvent is considered to be a structureless medium characterized only by its dielectric constant ϵ. ΔG_B is given by the following expression:

$$\Delta G_B = \frac{N_a q^2}{8\pi\epsilon_0 r}\left[\frac{1}{\epsilon_{hc}} - \frac{1}{\epsilon_w}\right]. \tag{8}$$

The second electrostatic contribution to the total free energy of transfer arises from image forces that originate from interactions of the ion with the water-lipid interfaces. Image forces occur when an ion located close to an interface in a solvent of dielectric constant ϵ_1 interacts with its induced "image" counterpart in a solvent of dielectric constant ϵ_2 on the other side of the interface. Several authors have described in detail how image energies of an ion inside a lipid bilayer can be quantified (Neumcke and Läuger, 1969; Parsegian, 1969; Flewelling and Hubbell, 1986b). For our purposes, we have chosen the approach outlined by Neumcke and Läuger. According to them, the image energy of an ion locted in a bilayer (ΔG_I) can be calculated as follows:

$$\Delta G_I = -\frac{N_a q^2 \vartheta}{16\pi\epsilon_0\epsilon_{hc}}\left[\frac{1}{x} + \frac{1}{d} \cdot \sum_{n=1}^{\infty}\left[\frac{\vartheta^{2n}}{n + x/d} + \frac{\vartheta^{2n-2}}{n - x/d} - \frac{\vartheta^{2n}}{n + r/d} - \frac{\vartheta^{2n-2}}{n - r/d}\right]\right] \tag{9}$$

where

$$\vartheta = \frac{\epsilon_w - \epsilon_{hc}}{\epsilon_w + \epsilon_{hc}}.$$

The sum in the expression above was found to converge rapidly and was terminated routinely at $n = 100$. Since the dielectric constant of the bilayer interior is always lower than the dielectric constant of water, the sign of the image energy term is negative and will therefore lower the total electrostatic energy. x denotes the distance of the ion from the water hydrocarbon interface. Since ΔG_I has a maximum if the ion is located at the center of the bilayer, we will use ΔG_I obtained for $x = d$ for further calculations. As compared to ΔG_B, ΔG_I is much less sensitive to the ionic radius and becomes increasingly negative if the thickness of the bilayer is decreased. In thin bilayers ($d \sim 20$ Å), the reduction of the Born energy by ΔG_I for an ion of radius 3.3 Å amounts to roughly 20% of its original value, resulting in a notable change in both K and P.

The observation that anions permeate much faster through bilayers than cations of comparable size indicates the presence of an internal dipole potential ($\Delta\phi$) in the bilayer, positive inside and negative outside (Flewelling and Hubbell, 1986a, b; Franklin and Cafiso, 1993). It is believed that dipole potentials are induced by the carbonyl groups of the lipids and that the values for $\Delta\phi$ are in the order of -200 to -280 mV. Another source of the dipole potential might be oriented water molecules that are tightly bound in the lipid headgroup region. The contribution of the dipole potential to the total Gibbs free energy is given by:

$$\Delta G_D = -qN_a\Delta\phi. \quad (10)$$

The sign of ΔG_D is negative for anions and positive for cations, lowering the energy barrier imposed by the bilayer for anions relative to cations. Strictly, Eq. 10 applies only for completely unhydrated ions (Volkov et al., 1997), such as the large, hydrophobic species studied by Flewelling and Hubbell (1986a, b). We will show below how the effects of hydration can be included for ordinary anions such as halides.

In addition to the electrostatic terms, we also include the energy contribution due to the hydrophobic effect. This takes into account the energy that is required to remove a spherical cavity of charge zero and radius r from the aqueous phase and place it in the hydrophobic phase of the bilayer interior. To compute this energy, Uhlig's equation is frequently used (Uhlig, 1937; Kornyshev and Volkov, 1984).

$$\Delta G_H = -N_a 4\pi r^2 \gamma_{w/hc} \quad (11)$$

Here, $\gamma_{w/hc}$ is the interfacial energy that equals the difference in surface energy of the aqueous and the hydrophobic medium. Although Uhlig's equation was developed for the hydration of inert gases, it also successfully accounts for the resolvation of molecules and ions between two liquid phases. Since $\gamma_{w/hc}$ is positive, ΔG_H is always negative, and therefore favors the partitioning of the ion into the bilayer. The contribution of ΔG_H to the total free energy of transfer is substantial and can outweigh the combined electrostatic terms in the case of very large ions.

Another factor that can affect the partition coefficient of an ion is the number and orientation of the water molecules in its hydration shell. One consequence of the presence of a hydration shell is the reduction of the effect of the dipole potential, $\Delta\phi$, due to screening of the electric field by the water molecules. In other words, a small, fully hydrated ion inside a bilayer will be less affected by a dipole potential than a large, hydrophobic ion. This issue becomes particularly interesting for the three halides, which possess practically identical hydrated radii (Conway, 1981), but differ in their bare radius. A second factor that is affected by the nature of the hydration shell is ion-specific interactions occurring at the lipid-water interface, in which water dipoles in the hydration shell interact with surface charges or dipoles located in the lipid headgroup region (polar lipid headgroups or tightly bound water molecules, for example). Again, the strength of these interactions will depend on the number and orientation of the water molecules in the hydration shell.

To include the effect of hydration in our calculations, we introduced an ion-specific energy term in Eq. 7, ΔG_{SP}. Since the exact magnitude of this term is difficult to assess, we restrict ourselves to a qualitative interpretation. Generally speaking, we expect ΔG_{SP} to partially compensate the effect of the dipole potential that is expressed in ΔG_D. Consequently, the sign of ΔG_{SP} will be positive for anions and negative for cations. We furthermore assume that the absolute value of ΔG_{SP} is directly related to the number of water molecules in the hydration shell.

By inserting the total Gibbs free energy of transfer in Eq. 5, we can now estimate permeability coefficients. More importantly, we can use this equation to plot P as a function of bilayer thickness, ionic radius, and sign of charge.

The pore mechanism

According to the pore mechanism, permeation of ions across a bilayer occurs through transient defects that are produced by thermal fluctuations (Nagle and Scott, 1978; Elamrani and Blume, 1983; Markin and Kozlov, 1985; Deamer and Nichols, 1989; Hamilton and Kaler, 1990a, b). By passing through hydrated pores in the bilayer, the permeant can largely circumvent the high energy cost required to partition into the hydrophobic region of the membrane (Parsegian, 1969). Naturally, the pathway described by this model is favored for permeants having low solubility in hydrophobic solvents so that pores can provide an alternative pathway for permeation. Apparently, permeation through pores becomes relevant for cations in thin bilayers (Deamer and Volkov, 1995; Paula et al., 1996).

In order to analyze this mechanism, we must develop an expression of P as a function of bilayer thickness, ionic radius, and sign of charge. A simplified model was proposed by Hamilton and Kaler (1990a, b). According to this description, the permeability coefficient can be expressed as a function of bilayer thickness and ionic radius using the following expression:

$$P = \frac{D_M \sigma n_o RT}{R_v A k_1}\left[\pi r^2 + \frac{RT}{k_1}\right]\exp\left[\frac{-k_1\pi r^2}{RT}\right]\exp\left[\frac{-k_2 d}{RT}\right]. \quad (12)$$

The parameters used in this equation are defined as follows: D_M is the diffusion coefficient of the permeating ion in water; σ is the surface concentration enhancement due to electric double layers at the lipid-water interface; A is the bilayer surface; R_v is the radius of the liposome; R is the gas constant; T is temperature; n_o is the maximum pore number; r is the unhydrated radius of the permeating ion; and d is the thickness of the hydrophobic part of the bilayer. The constants k_1 and k_2 refer to the energy associated with the formation of a pore of radius r and depth d, respectively. The values for k_1 and k_2 were obtained by Hamilton and

Kaler from curve fits of Eq. 12 to their set of experimental data, which were collected for cations in vesicles made from synthetic surfactants.

It should be emphasized that this model is based on the assumption that permeation occurs through hydrated, hydrophilic defects. This implies that the ion remains hydrated as it passes through a pore and that the water molecules in the hydration shell of an ion are replaced by water molecules bound to the lipid headgroups. Therefore, bare ionic radii rather than hydrated radii are used in Eq. 12.

Another parameter that has important implications for the following discussion is the surface concentration enhancement σ. This parameter accounts for the effects of electric double layers at the water-lipid interface. Hamilton and Kaler specified σ with a value of 10 for cations in bilayers made from synthetic surfactants with negatively charged headgroups. Accordingly, a factor of 0.1 should apply for anions. Since the PC used in our study are zwitterionic rather than negatively charged, the use of this particular value for σ is debatable. Nevertheless, even in the case of liposomes composed of zwitterionic PC, σ is expected to be >1 for cations and <1 for anions. This effect is caused by the dipole moments of the lipid headgroups and bound water molecules (see previous section) that have their negative centers of charge oriented toward the aqueous phase and thereby increase the cation concentration at the interface relative to the bulk. As a result, the permeability coefficient for cations will be higher than for anions. This qualitative assessment is sufficient for our discussion of the influence of the sign of ionic charge because σ is the only factor in the pore mechanism that discriminates between cations and anions. Equation 12 represents the counterpart to Eq. 5 and permits the calculation of P as a function of d, r, and sign of charge.

Comparison of the two mechanisms

With the aid of the theory outlined above, we will now compare and discuss the predictions that the two mechanisms make for P with respect to the experimental variables membrane thickness, ionic radius, and sign of charge. Table 2 summarizes the major findings.

TABLE 2 Comparison of the parameter sensitivity of the solubility-diffusion and the pore mechanism

Parameter	Solubility-Diffusion Mechanism	Pore Mechanism
Sign of ionic charge (±)	$P_{anion} > P_{cation}$	$P_{cation} > P_{anion}$
Bilayer thickness d	P varies moderately with d	P varies strongly with d
Ionic radius r	P generally increases with increasing ionic radius	P decreases with increasing ionic radius

The influence of sign of charge

The crucial factor in the solubility-diffusion mechanism that clearly differentiates between cations and anions is the dipole potential $\Delta\phi$, expressed in terms of ΔG_D. For simplicity, we will not explicitly include the effect of ΔG_{SP} at this point, but describe its effect by operating with a slightly reduced dipole potential (-150 mV instead of ~ -240 mV). This is justified since ΔG_{SP} will only counteract a certain fraction of ΔG_D, but never fully compensate for it (see discussion above). Fig. 3 nicely illustrates the tremendous changes in P that are caused by the dipole potential. The difference between ions that have the same hydrated radius but a different sign of charge is 3 to 4 orders of magnitude. This is the difference observed between potassium and halide permeability coefficients in experiments.

This characteristic is obviously inconsistent with the pore mechanism. Here, the relevant parameter that is sensitive to the sign of ionic charge is the surface concentration enhancement factor σ. As pointed out above, σ is greater for cations than for anions, causing the permeability coefficient to be smaller for anions than for cations. Using values of 10 and 0.1 as an approximation (Hamilton and Kaler, 1990a), the difference is two orders of magnitude. Thus, the experimental data clearly favor the solubility-diffusion mechanism.

The influence of bilayer thickness

Fig. 3 presents experimentally determined and calculated permeability coefficients as a function of bilayer thickness on a semi-logarithmic scale. The curve obtained from the pore mechanism is a straight line with a slope given by the constant k_2. The solubility-diffusion mechanism produces a line differing from the previous one in two respects. First, the slope is not constant but instead depends on d, with a steeper slope for thin bilayers than for thicker ones. Second, the slope of the line produced by the solubility-diffusion curve is always less than that predicted by the pore mechanism, even for thin bilayers. Since the experimental data for halide permeability coefficients exhibit a rather modest dependence of P on d, the experimental data support a solubility-diffusion mechanism and argue against permeation through pores.

The influence of ionic radius

Fig. 4 illustrates how P is affected by the radius of the permeating ion at a fixed bilayer thickness of 30 Å. It should be reemphasized that unhydrated radii are used in conjunction with the pore mechanism whereas the hydrated radii are used for the solubility-diffusion mechanism. An obvious feature is that the pore mechanism is dramatically less sensitive to changes in the ionic radius than the solubility-diffusion mechanism. Since the unhydrated radius increases in the order $r_{Cl} < r_{Br} < r_I$, the permeability coefficient as predicted by the pore mechanism should decrease very moderately in the same order ($P_{Cl} > P_{Br} > P_I$). The

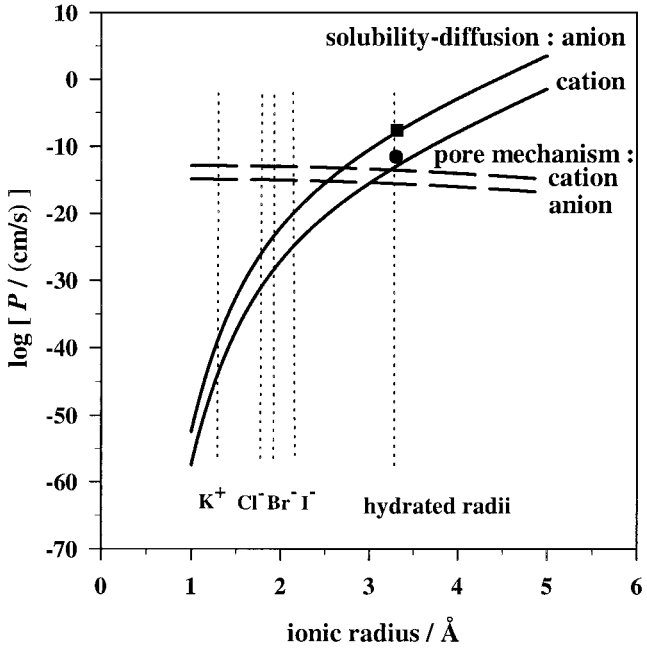

FIGURE 4 Dependence of P on ionic radius. Experimentally determined permeability coefficients of potassium (●) and the halides (■; the points for chloride, bromide, and iodide coincide on this scale, if hydrated radii are used). The solid lines were obtained from Eq. 5 for the solubility-diffusion mechanism (upper line for an anion, lower line for a cation). The dashed line was computed from Eq. 12 according to the pore mechanism (parameters as in Fig. 3).

experimental results, however, indicate that exactly the opposite is the case.

Fig. 4 also reveals why only hydrated radii are reasonable parameters in conjunction with the solubility-diffusion mechanism. Bare radii yield values for P that are many orders of magnitude lower than the experimental findings. Furthermore, the calculated differences between the halide permeability coefficients are too large.

Since the hydrated radii for the three halides are virtually the same (3.31 Å; Conway, 1981), the solubility-diffusion mechanism predicts identical P values, if ΔG_{SP} is neglected. Before we include this energy term in our discussion, it should be noted that the sensitivity of the two mechanisms with respect to the ionic radius by itself already points to the solubility-diffusion mechanism. Keeping in mind how sensitive P is to the ionic radius, it is clear that minor changes in this parameter will cause dramatic changes in the calculated permeability coefficient, as illustrated in Fig. 4. Given the uncertainties that are attached to the measurements of hydrated ionic radii, a difference of only 0.1 Å can easily account for the relatively small difference in the experimental values for P between the individual halides. It should be noted that a similar argument cannot be made for the pore mechanism. Due to the insensitivity of the pore mechanism, unrealistically large differences in the unhydrated (!) ionic radii would be required to explain the experimentally observed differences in permeation rates.

We will now include ΔG_{SP} in our calculation. As stated above, the exact value of ΔG_{SP} is unknown, but it will be largest for chloride, which has the largest hydration shell and smallest for iodide. The sign of ΔG_{SP} is positive, reducing the effect of ΔG_D. As a consequence, the permeability coefficients for the halides will increase in the order $P_{Cl} < P_{Br} < P_I$, which is exactly what is observed. Fig. 5 represents an attempt to select ΔG_{SP} in order to account for the differences in the permeability coefficients of the halides. Potassium ion data were also included also in this Fig. 5. The selected values for ΔG_{SP} were 10 kJ/mol for chloride, 5 kJ/mol for bromide, 0.5 kJ/mol for iodide, and −16 kJ/mol for potassium ions, if the value of the dipole potential was selected to be −240 mV. Alternatively, one could account for the effect of the hydration shell by using a dipole potential specifically reduced for each ion, which would amount to −136 mV for chloride, −188 mV for bromide, −234 mV for iodide, and −74 mV for potassium ions. Both of our previously stated requirements for ΔG_{SP} are fulfilled throughout this procedure: the absolute value of ΔG_{SP} increases with the number of hydrating water molecules ($I^- < Br^- < Cl^- < K^+$) and the sign of ΔG_{SP} changes as the sign of the ionic charge changes.

SUMMARY

We conclude from our analysis that the solubility-diffusion mechanism better describes permeation of halide ions across phospholipid bilayers than the pore mechanism. We base our argument on the experimentally observed dependence of the permeability coefficients on the sign of the

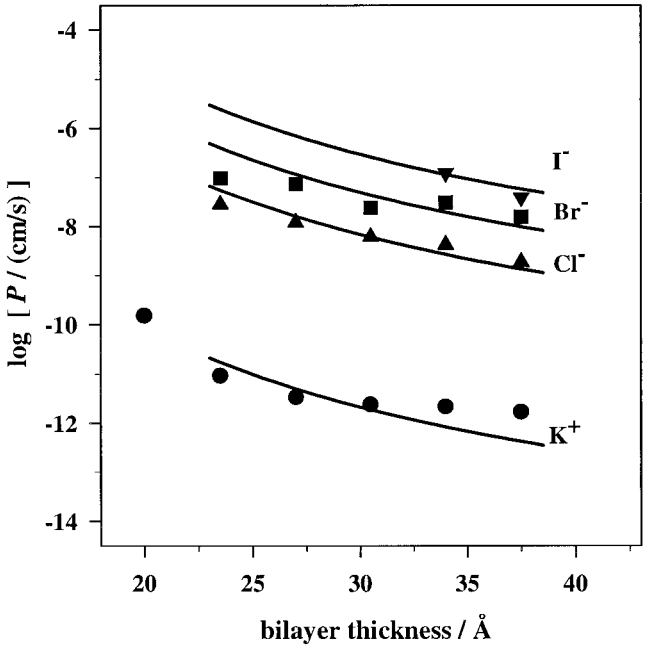

FIGURE 5 Experimentally determined permeability coefficients and theoretical lines derived from the solubility-diffusion mechanism, including the effect of the hydration shell. Parameters are the same as in Fig. 3 with the following exceptions: $\Delta\phi = -240$ mV, ΔG_{SP} (K^+) = −16.0 kJ/mol, ΔG_{SP} (I^-) = 0.5 kJ/mol, ΔG_{SP} (Br^-) = 5.0 kJ/mol, ΔG_{SP} (Cl^-) = 10.0 kJ/mol.

ionic charge, on the bilayer thickness, and on the ionic size. In each case, the comparison of the experimental evidence to theoretical predictions supported the solubility-diffusion mechanism and was inconsistent with permeation through pores.

This work was supported by National Aeronautics and Space Administration Grant NAGW-4235.

REFERENCES

Born, M. 1920. Volumen und Hydrationswärme der Ionen. *Z. Phys.* 1: 45–48.

Conway, B. E. 1981. Ionic Hydration in Chemistry and Biophysics. Elsevier, New York.

Deamer, D. W., and J. W. Nichols. 1989. Proton flux mechanisms in model and biological membranes. *J. Membr. Biol.* 107:91–103.

Deamer, D. W., and A. G. Volkov. 1995. Proton permeation of lipid bilayers. *In* Permeability and Stability of Lipid Bilayers. E. A. Disalvo and S. A. Simon, editors. CRC Press, Boca Raton, Florida. 161–177.

Dilger, J. P., S. G. A. McLaughlin, T. J. McIntosh, and S. A. Simon. 1979. The dielectric constant of phospholipid bilayers and the permeability of membranes to ions. *Science.* 206:1196–1198.

Elamrani, K., and A. Blume. 1983. Effect of the lipid phase transition on the kinetics of H^+/OH^- diffusion across phosphatidic acid bilayers. *Biochim. Biophys. Acta.* 727:22–30.

Finkelstein, A. 1987. Water Movement through Lipid Bilayers, Pores, and Plasma Membranes: Theory and Reality. Wiley Interscience, New York.

Flewelling, R. F., and W. L. Hubbell. 1986a. Hydrophobic ion interactions with membranes: thermodynamic analysis of tetraphenylphosphonium binding to vesicles. *Biophys. J.* 49:531–540.

Flewelling, R. F., and W. L. Hubbell. 1986b. The membrane dipole potential in a total membrane potential model. *Biophys. J.* 49:541–552.

Franklin, J. C., and D. S. Cafiso. 1993. Internal electrostatic potentials in bilayers: measuring and controlling dipole potentials in lipid vesicles. *Biophys. J.* 65:289–299.

Gennis, R. B. 1989. Biomembranes: Molecular Structure and Function. Springer Verlag, New York 241–247.

Gurney, R. W. 1953. Ionic Processes in Solution. Dover Publications, New York.

Gutknecht, J., J. S. Graves, and D. C. Tosteson. 1978. Electrically silent anion transport through lipid bilayer membranes containing a long-chain secondary amine. *J. Gen. Physiol.* 71:269–284.

Hamilton, R. T., and E. W. Kaler. 1990a. Alkali metal ion transport through thin bilayers. *J. Phys. Chem.* 94:2560–2566.

Hamilton, R. T., and E. W. Kaler. 1990b. Facilitated ion transport through thin bilayers. *J. Membr. Sci.* 54:259–269.

Hauser, H., D. Oldani, and M. C. Phillips. 1973. Mechanism of ion escape from phosphatidylcholine and phosphatidylserine single bilayer vesicles. *Biochemistry.* 12:4507–4517.

Hope, M. J., M. B. Bally, G. Webb, and P. R. Cullis. 1985. Production of large unilamellar vesicles by a rapid extrusion procedure: characterization of size distribution, trapped volume, and ability to maintain a membrane potential. *Biochim. Biophys. Acta.* 812:55–65.

Israelachvili, J. N. 1992. Intermolecular and Surface Forces. Academic Press, San Diego.

Ketterer, B., B. Neumcke, and P. Läuger. 1971. Transport mechanism of hydrophobic ions through lipid bilayer membranes. *J. Membr. Biol.* 5:225–245.

Kornyshev, A. A., and A. G. Volkov. 1984. On the evaluation of standard Gibbs energies of ion transfer between two solvents. *J. Electroanal. Chem.* 180:363–381.

Lakowicz, J. R. 1983. Principles of Fluorescence Spectroscopy, Chap. 9. Plenum Press, New York and London.

Lewis, B. A., and D. M. Engelman. 1983. Lipid bilayer thickness varies linearly with acyl chain length in fluid phosphatidylcholine vesicles. *J. Mol. Biol.* 166:211–217.

Markin, V. S., and M. M. Kozlov. 1985. Pore statistics in bilayer lipid membranes. *Biol. Mem.* 2:404–442.

Markin, V. S., and A. G. Volkov. 1989. The Gibbs free energy of ion transfer between two immiscible liquids. *Electrochim. Acta.* 34:93–107.

Marrink, S. J., and H. J. C. Berendsen. 1994. Simulation of water transport through a lipid membrane. *J. Phys. Chem.* 98:4155–4168.

Nagle, J. F., and H. L. Scott. 1978. Lateral compressibility of lipid mono and bilayers. Theory of membrane permeability. *Biochim. Biophys. Acta.* 513:236–243.

Neumcke, B., and P. Läuger. 1969. Nonlinear electrical effects in lipid bilayer membranes. II. *Biophys. J.* 9:1160–1969.

Nicholls, P., and N. Miller. 1974. Chloride diffusion from liposomes. *Biochim. Biophys. Acta.* 356:184–198.

Parsegian, A. 1969. Energy of an ion crossing a low dielectric membrane: solutions to four relevant electrostatic problems. *Nature*. 221:844–846.

Paula, S., A. G. Volkov, A. N. Van Hoek, T. H. Haines, and D. W. Deamer. 1996. Permeation of protons, potassium ions, and small polar molecules through phospholipid bilayers as a function of membrane thickness. *Biophys. J.* 70:339–348.

Small, D. M. 1967. Phase equilibria and structure of dry and hydrated egg lecithin. *J. Lipid Res.* 8:551–557.

Tanford, C. 1980. The Hydrophobic Effect: Formation of Micelles and Biological Membranes, Chap. 2. John Wiley and Sons, New York.

Toyoshima, Y., and T. E. Thompson. 1975. Chloride flux in bilayer membranes: chloride permeability in aqueous dispersions of single-walled, bilayer vesicles. *Biochemistry*. 14:1525–1531.

Uhlig, H. H. 1937. The solubilities of gases and surface tension. *J. Phys. Chem.* 41:1215–1225.

Verkman, A. S. 1990. Development and biological applications of chloride-sensitive fluorescent indicators. *Am. J. Physiol.* 259:C375–C388.

Verkman, A. S., M. C. Sellers, A. C. Chao, T. Leung, and R. Ketcham. 1989a. Synthesis and characterization of improved chloride-sensitive fluorescent indicators for biological applications. *Anal. Biochem.* 178: 355–361.

Verkman, A. S., R. Takla, B. Sefton, C. Basbaum, and J. H. Widdicombe. 1989b. Quantitative fluorescence measurement of chloride transport mechanisms in phospholipid vesicles. *Biochemistry*. 28:4240–4244.

Volkov, A. G., S. Paula, and D. W. Deamer. 1997. Two mechanisms of permeation of small neutral molecules and hydrated ions across phospholipid bilayers. *Bioelectrochem. Bioenerg.* 42:153–160.